RISE 4 – R/V Pt Sur Cruise Report
Leg 2, 2-12 June 2006

By David A. Jay, Jiayi Pan and Keith Leffler PSU
Alex Horner-Devine and Emily Spahn, UW
Jay Peterson, NOAA Fisheries,
Philip Orton, Lamont-Doherty and Greg Avicola OSU

Emily Spahn, UW

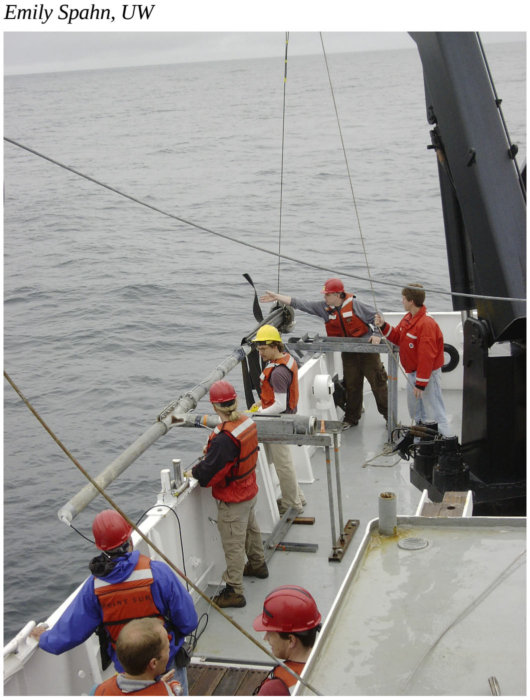

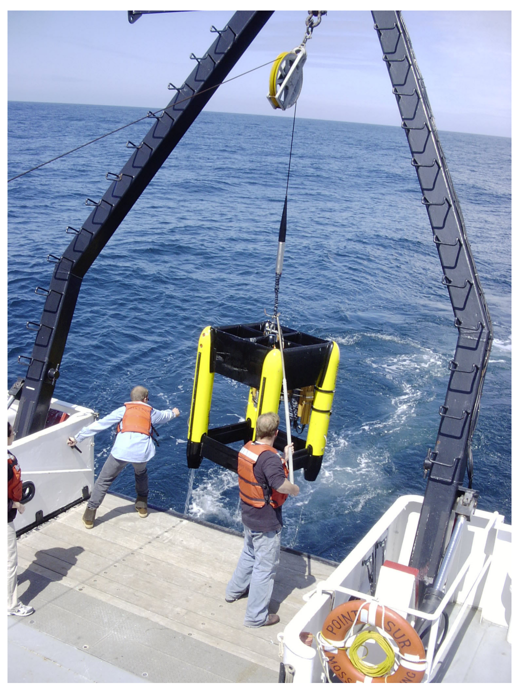

Purpose and Context

RISE hypothesizes that the Columbia River plume is more productive than adjacent coastal waters, that it facilitates cross-margin transport of particles and biota, and that the iron supplied by the plume is important to Pacific Northwest coastal primarily production, especially off Washington. Understanding the impact of the highly mobile Columbia River plume on coastal production and transport patterns requires that measurements be made on a variety of scales from turbulence to internal waves and fronts, to those of the plume and the underlying shelf circulation. RISE emphasizes, therefore, rapid surveys with the Triaxus towfish and detailed process investigations.

The RISE field program consists of two high-flow cruises (spring 2005 and 2006), one medium-flow cruise (July 2004) and one low-flow cruise (August 2005). Each cruise is to be carried out by two vessels, the R/V Wecoma (biological and chemical studies) and the R/V Pt Sur (plume surveys, mixing processes and zooplankton dynamics).

The first RISE cruise (RISE 1) in July 2004 was partially an exploratory venture, testing our approach to project hypotheses, and the suitability of sampling gear to the environments. An important conclusion from RISE 1 was that the turbulence and Triaxus sampling modes were fundamentally incompatible. Thus, 2005 sampling consists of one Triaxus cruise (RISE 2, June 2005) and one turbulence cruise (RISE 3, August 2003).

RISE 4 took place 21 May to 12 June 2006. This report covers the Leg 2 of that cruise, from 2 to 12 June 2006. Spring 2006 Columbia River flows were somewhat above long-term average, peaking at about 11,400 m^3s^{-1} at The Dalles and 12,700 m^3s^{-1} at Beaver (Figure 1). The dates of the peak flow at Beaver were 30-31 May, just before Leg 2. Westside flows were somewhat above average in late May due to above-average rainfall in May, concentrated in the last 10 days of the month (Figure 1). One interesting feature of this freshet was the fact that the Snake (22 May at Anatone, but later at Pasco) and Upper Columbia (28 May at Priest Rapids) peaks occurred almost simultaneously, whereas the Snake River peak often occurs several weeks before the Upper Columbia peak. The Snake has a relatively high sediment load, though this has been reduced by the four dams in the lower Snake River. The turbidity peak at Beaver was several days after the flow peak on 3 June (Figure 1b), the reasons for this are unclear. The Willamette exhibited two peaks, one 29 May at Salem (1-2 days later at Portland) and one 6 June. The second peak may have been associated with precipitation.

Winds during the cruise period (Julian days 152-162) were mostly to the north (downwelling favorable) and weak (up to d 156; Figure 2). This continued the conditions that prevailed during Leg 1, though winds were stronger for part of leg 1. Winds switched to upwelling favorable on 3 June, a condition that prevailed for the remainder of the cruise. Winds were not strong enough, however, to produce a strong surface expression of upwelled water, especially given the strong buoyancy input.

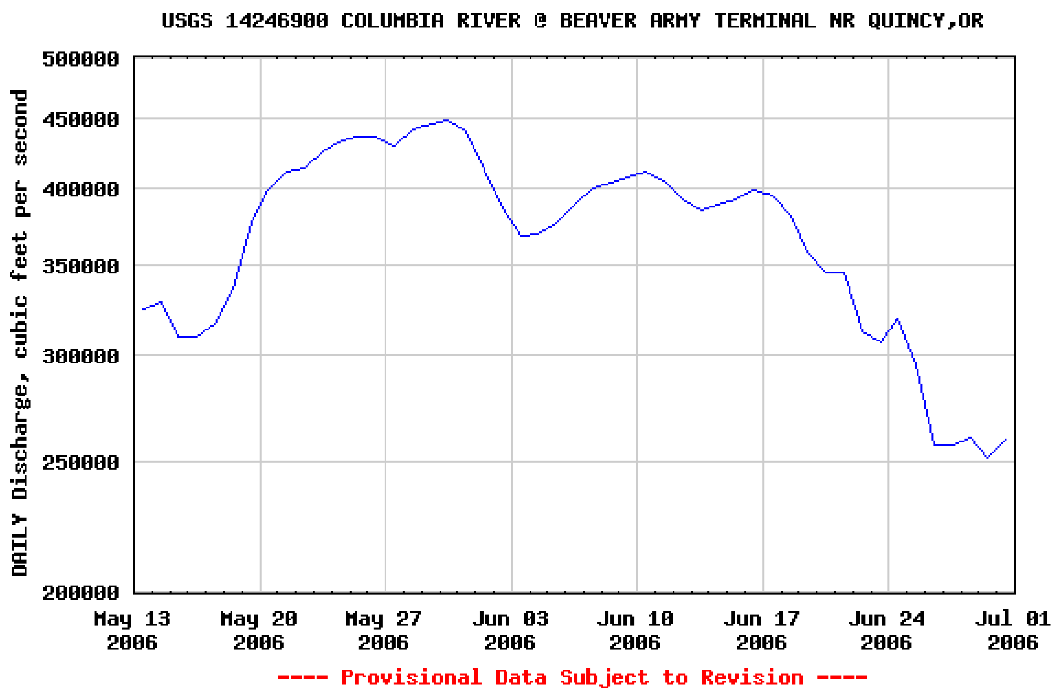

Figure 1a: *Columbia River flow in cfs at Beaver, from http://waterdata.usgs.gov/nwis/. The peak flow occurred 30-31 May.*

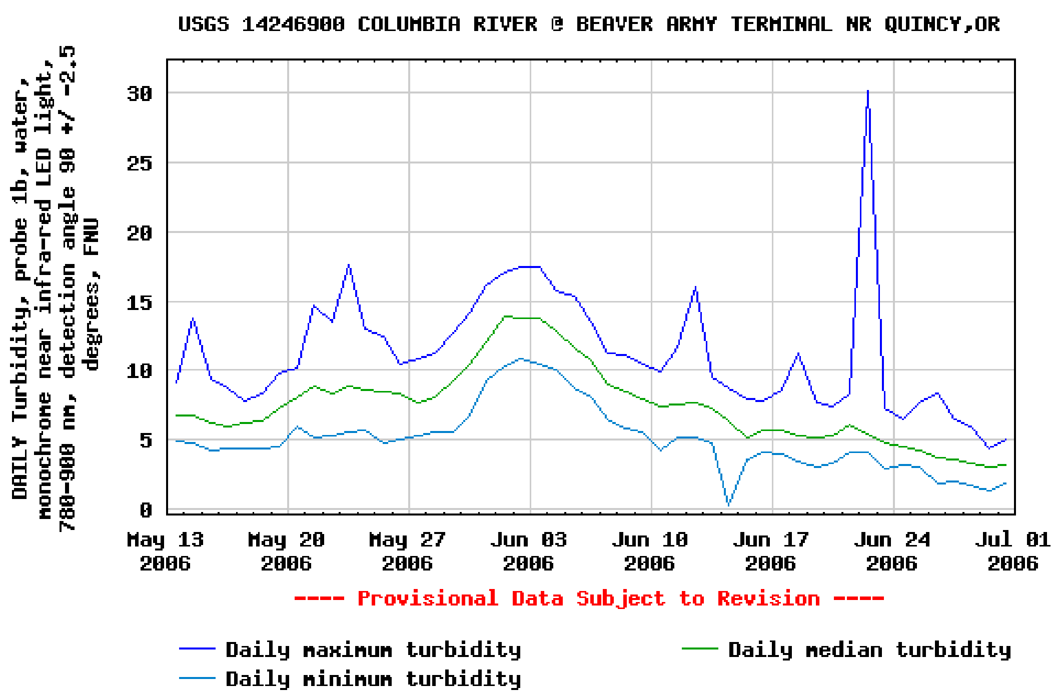

Figure 1b: *Columbia River turbidity in ftu at Beaver, from http://waterdata.usgs.gov/nwis/. The peak turbidity occurred 3 June.*

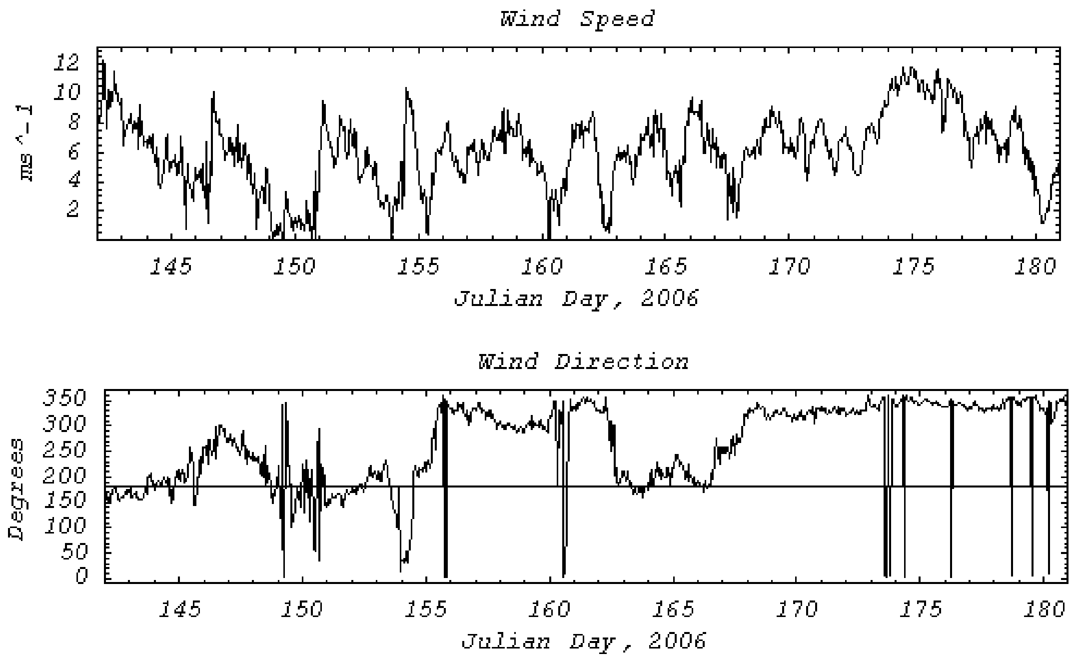

Figure 2: Wind speed and direction observed at NOAA 46029, from www.ndbc.noaa.gov/station_history.php?station=46029.

Three RISE research groups carried out work on the R/V Pt Sur during Rise 2001:

1) The Jay group from Portland State University (David A. Jay, Jiayi Pan, Greg Avicola, Keith Leffler, Philip Orton and Frank Opila) carried out Triaxus (Figure 3) surveys of the plume and studies internal waves, tides, vertical mixing, and fronts. The goals of this part of the project include describing the diverse physical processes occurring in the plume on scales (from vertical mixing to plume circulation), understanding the dynamics of internal waves, tides and fronts in the plume, and determining how these diverse, multi-scale processes contribute to productivity in the plume ecosystem Triaxus surveys characterize the plume-scale fields of near-surface velocity, salinity, temperature, nitrate, chlorophyll a, transmissivity, optical particle size and zooplankton characteristics. Large-scale maps were carried out under variable conditions at the beginning and end of the cruise. Frontal surveys were carried out during neap and spring tides, but primarily on spring tides. Observations of the plume lift-off zone were carried out with intermediate tidal forcing. Because of the lack of upwelling conditions, northerly fronts were not as strong as in 2004, but western fronts were very active in spawning internal waves.
2) The Peterson group (Dr. Bill Peterson, Leah Feinberg, Tracy Shaw, Jennifer Menkel and Jay Peterson) is investigating the distribution, abundance, and species composition of mesozooplankton in proximity to the Columbia River plume. A two-component approach is used to study the spatial variation of zooplankton species and life stages as well as their rates of growth, grazing, and mortality associated with the coastal regions impacted by the Columbia River plume. The first component focuses on rate processes and involves net sampling and live organism incubations aboard the R/V Wecoma (see the R/V Weco-

ma cruise report). The second component consists of high resolution surveys of plankton distribution and size carried out using a Laser Optical Plankton Counter (LOPC) carried by the *R/V Pt. Sur* Triaxus. The LOPC gathers data on the abundance and distribution of particles between 100 μm and 35 mm in equivalent spherical diameter (ESD) throughout the region surveyed by the Triaxus. Zooplankton size and abundance data are gathered real-time in association with GPS, salinity, temperature, depth and fluorescence data. Vertical net tows (0.5m diameter net with 153 μm mesh) were periodically taken during the survey to collect zooplankton for species identification.

3) The UW Civil and Environmental Engineering group (Alex Horner-Devine and Emily Spahn) conducted Triaxus surveys of the plume and frontal studies in coordination with the Jay group, but with an emphasis on particle properties deduced from the LISST-100, LISST-25 and bottle samples. The primary objective of this work is to measure the time-varying particle distribution in the near-field of the plume and identify mechanisms that lead to this observed distribution. The observed spatial and temporal variability will be compared with variability in other measured plume parameters such as micronutrient concentration and productivity in order to determine the role that particles play in the plume-influenced coastal ecosystem. Another area of interest is the rate of growth of the initial plume bulge and the transition to a coastal flow on the downstream side.

RISE 4 Personnel

	Name	Institution	Position (chief scientist., student, technician, etc.)	Dates on Board
1	David Jay	PSU	Chief Scientist	6/1-6/12
2	Alex Horner-Devine	UW	Scientist	6/1-6/12
3	Jay Peterson	OSU	Scientist	6/1-6/12
4	Jiayi Pan	PSU	Scientist	6/1-6/12
5	Greg Avicola	OSU and PSU	Scientist	6/1-6/12
6	Philip Orton	Lamont-Doherty	Graduate Student	6/1-6/12
7	Keith Leffler	PSU	Graduate Student	6/1-6/12
8	Emily Spahn	UW	Graduate Student	6/1-6/12
9	Frank Opilia	PSU	Temporary staff	6/1-6/12

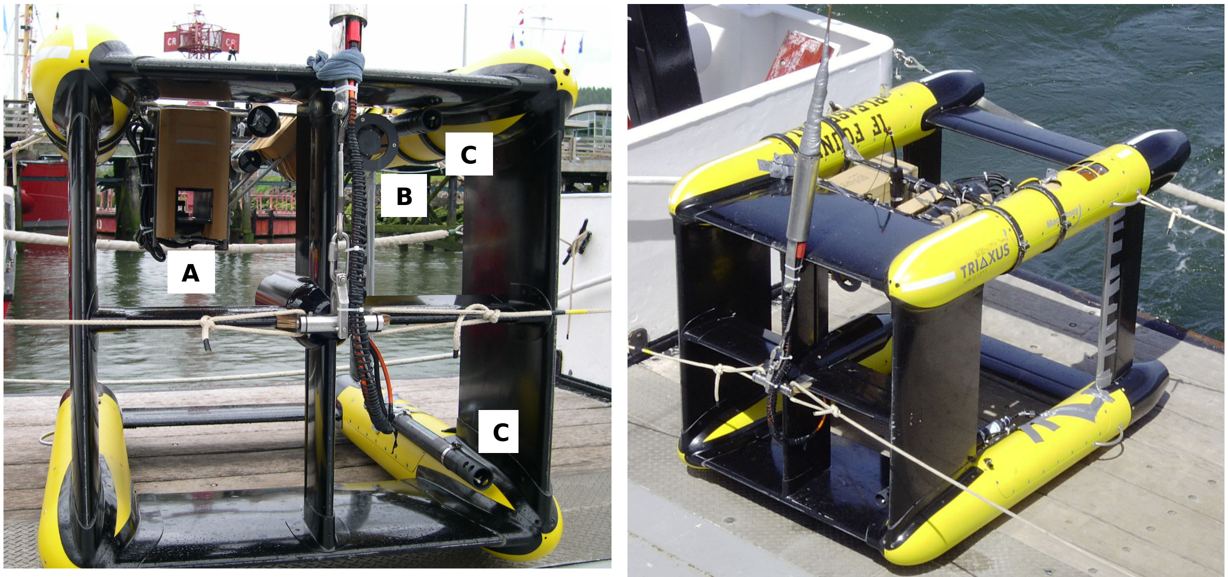

Figure 3a,b: At left in a), two views of the Triaxus towfish, showing the LOPC (A), LISST-100 (B) and the two OS-200 CTDs (C). The Remus-configuration 1200 kHz ADCP is mounted in the top right pontoon and looks upward; it is visible at right in b).

Figure 3c,d: At left in c) a close-up of ADCP head. At right in d) the pole-mounted Remus 1200 kHz ADCP (shown with pole retracted for transport). The first bin of good data is at 3.7 m nominal depth.

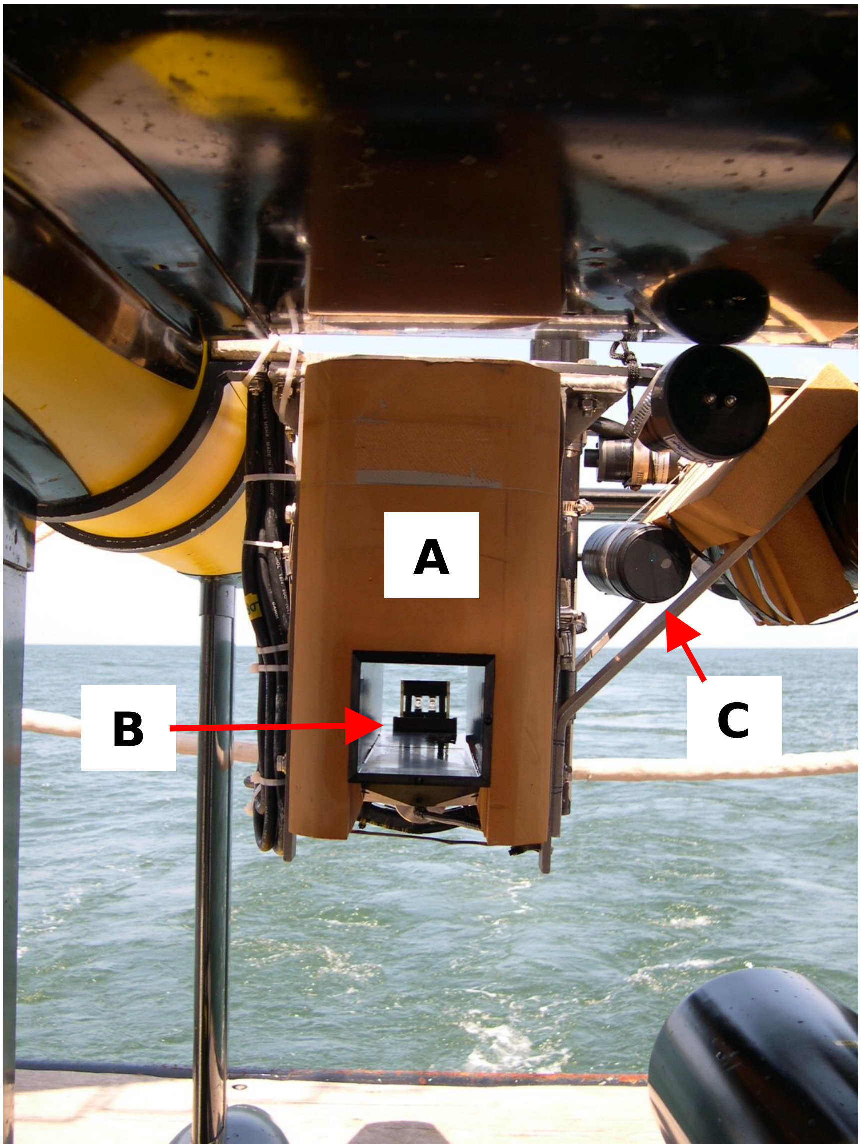

Figure 4: Detail of the LOPC as mounted on Triaxus: (A) with its attached conductivity, temperature, depth sensor (B) mounted at the rear of the LOPC sampling tunnel, and fluorometer calibrated for chlorophyll a (C).

RISE-4 Pt Sur Schedule

Date/Time, PDT	**Pt Sur Activity**
6/1 0800	Stage in Newport
	BEGIN CRUISE
6/2 1000 to 1300	Depart from Newport to sea, 40 m depth; lower ADCP pole; do plankton tow and CTD cast; bottles for N and SPM; put in Triaxus; safety drill
Map 1	**Map 1: Initial large-scale Triaxus map (see figure)**
6/2 ~1130 to 6/4 1800	downwelling configuration was run, using shortened lines, because of absence of a southerly plume. Much of map was aborted due to Triaxus malfunctions
	Long Beach Line at 46º 30′ N
6/4 1800 to 6/6 2200	Put in Triaxus and do Triangle Map
	Plume Axis Drift May
6/7 0200 to 6/8 0900	Put in Triaxus and run 46-14 Line during the day and NS-line during dark hours, if crab pots allow.
6/9 0900	Pull Triaxus and do CTD cast at CR buoy
	RT to Astoria
6/8 1100 to 6/8 1900	Transit to Astoria from CR buoy, pick up replacement LOPC, return to CR buoy
	NS Line
6/8 2100	Do CTD cast and net tow at N. end of NS Line (WP 3)
6/8 2300 to 6/9 0600	Sample NS Line from WP-1 to WP-3; Triaxus damaged by crab pot
	RT to Astoria
6/9 1100 to 6/9 1700	Transit to Astoria from CR buoy, machine work and parts for Triaxus, return to CR buoy
	NS Line
6/9 1900 to 6/10 1000	Sample NS Line from WP-1 to WP-3; Triaxus catches crab pot; two hours lost in early morning
	Final Map from Grays Harbor to Cape Meares
6/10 0900 to 6/12 0400	Final Map
6/12 0400	Pull Triaxus and pole, do CTD and net tow
6/12 0800 to 6/12 1400	**Steam to Newport**
	END OF CRUISE
	Start Northern Fronts and IW
6/9 2000 to 6/11 2200 (50 hrs)	Put in Triaxus and run Long NS Line with extension to N during daylight hours, regular NS Line in dark hours
6/11 2200 to 6/12 0030 (2.5 hrs)	Pull Triaxus, do CTD cast with bottles and plankton tow at NS Line WP 2. Pull ADCP
	End Northern Fronts and IW
6/12 0030 to 6/12 1430 (14 hours)	Return to Newport
	END OF CRUISE

List of Sensors/Data Sets Acquired

Shipboard:

1) Vessel 300 kHz RDI acoustic Doppler current profiler (ADCP), downward looking: profiles of horizontal velocity, 1 m bins.
2) Vessel 300 kHz RDI acoustic Doppler current profiler (ADCP), downward looking: profiles of horizontal velocity,4 m bins.
3) Pole-mounted 1200 kHz RDI (Remus) ADCP with Mode 12 firmware, downward looking: profiles of horizontal velocity, 0.25 or 0.5 m bins.
4) Pole mounted OS-200 CTD: conductivity, temperature, depth and OBS (optical backscatter) at 1 m nominal depth.
5) Underway data acquisition system (UDAS), Seabird 911 CTD with transmissometer and fluorometer: conductivity, temperature, optical transmission, and chlorophyll a at 3 m nominal depth.
6) Vessel radar acquired as jpeg images at 1 image minute^{-1}.
7) CTD casts:
    a. Seabird 911 CTD with transmissometer and fluorometer; conductivity, temperature, depth, optical transmission, and chlorophyll a.
    b. Laser in-situ scattering transmissometer, LISST-25; volume concentration in two size bins, 3-62.5 and 62.5 to 500 micron.
    c. Bottle samples for total SPM, nutrients, and chlorophyll a.

Triaxus Tow Fish:

1) Seabird 911 CTD with transmissometer, fluorometer, ISUS NO_3 sensor; conductivity, temperature, depth, optical transmission, chlorophyll a, and $N0_3$.
2) 1200 kHz RDI (Remus) ADCP with Mode 12 firmware, upward looking; high resolution, near-surface horizontal velocity profiles
3) Laser-optical plankton counter (LOPC); abundance and distribution of particles between 100 μm and 35mm in equivalent spherical diameter (ESD).
4) LISST-100; volume concentration in 32 size bins, 10-1,500 micron
5) Two OS-200 CTDs; conductivity temperature and depth (for stratification and vertical mixing from fine structure).

Selected Results

1. Regional-Scale Plume Maps:

Two large-scale maps were planned for RISE4 Leg 2, but due to Triaxus problems, only one full map was run, 10-12 June under prolonged, weak upwelling favorable winds. However, a partial map was run between approximately Long Beach (46º 30′) and Cape Meares (46º 29.95′) resulted from a plume axis study on 7-8 June. Because of the strength of regional stratification caused by the high river flow during May, little or no upwelling occurred during this map. Surface salinity, chl a (as fluorescence), and transmissivity from the Pt Sur UDAS (underway data acquisition system) are shown in Figure 5a-c for the partial map. Although little or no upwelling was occurring, the plume moved generally south, along with a large mass of low salinity water that was originally pushed northward along the Washington Coast during downwelling conditions. This older freshwater is seen to the west of the new plume water, yield a “sock” plume.

Much of the final map (10-12 June 2006) was run in a boustrophedonic or zig-zag pattern (Figure 6). Upwelling favorable-winds had been present for almost a week at the time of this survey. Although Figure 6 shows the plume in a typical southerly upwelling configuration, no upwelling is believed to have been occurred before 11 June. Upwelling may have begun on 11-12 June. (Our detection of upwelling may have been incomplete, however, because of our inability to sample inshore of 100 m, due to crab pots.) The likely reasons for the absence of actual upwelling were: a) the fact the upwelling-favorable winds were relatively weak, and b) high ambient stratification throughout the survey area due to high river flows during May. This upwelling may have been captured at the very southeast end of the line, off Newport. As is typical for a sourtherly plume, old plume water that was originally N of the entrance (seen in Figure 5 between 45.9 and 46.2 º N) is moving south in seaward of the new plume water mass. In Figure 6, this old plume water has moved south to 45.65º N and may extend even further south. It is notable that production (as judged by chl-a) is seen primarily in new and old plume water. The onset of production may have been captured off Newport, however.

2. <u>Frontal Processes</u>

Fronts are an important plume environment, and a variety of fronts are observed in the plume area. These fronts accumulate particles and organisms, may exhibit high vertical mixing rates, and support feeding by seabirds and juvenile salmonids. Strong tidal currents and buoyancy input sometimes cause these fronts to exhibit large density contrasts (□S >20 over <150 m), sharp convergence (□U >0.5 ms^{-1} over <150 m), and rapid propagation (sometimes in excess of 1 ms^{-1}). Such fronts provide a productive habitat where zooplankton, birds and juvenile salmonids congregate. Frontal mixing also assists in maintaining plume productivity despite high ambient stratification (Orton and Jay, 2005). Frontal types include:

a. V-shaped salinity intrusion fronts inside the estuary mouth on flood.

b. Lateral fronts bounding the estuarine outflow; these are especially prominent on greater ebbs and cause considerable mixing.

c. North and northwestern fronts propagating into high salinity, relatively weakly stratified waters. These fronts exhibit very strong convergence, especially when they propagate against ambient coastal flow that is to the south under upwelling conditions. Accordingly, these were found to be stronger in 2004 than in 2005; they were not observed at all in 2006. These fronts cause very strong mixing (Orton and Jay, 2005) and may spawn soliton trains (Nash and Moum, 2005), if there is sufficient stratification in the ambient ocean waters.

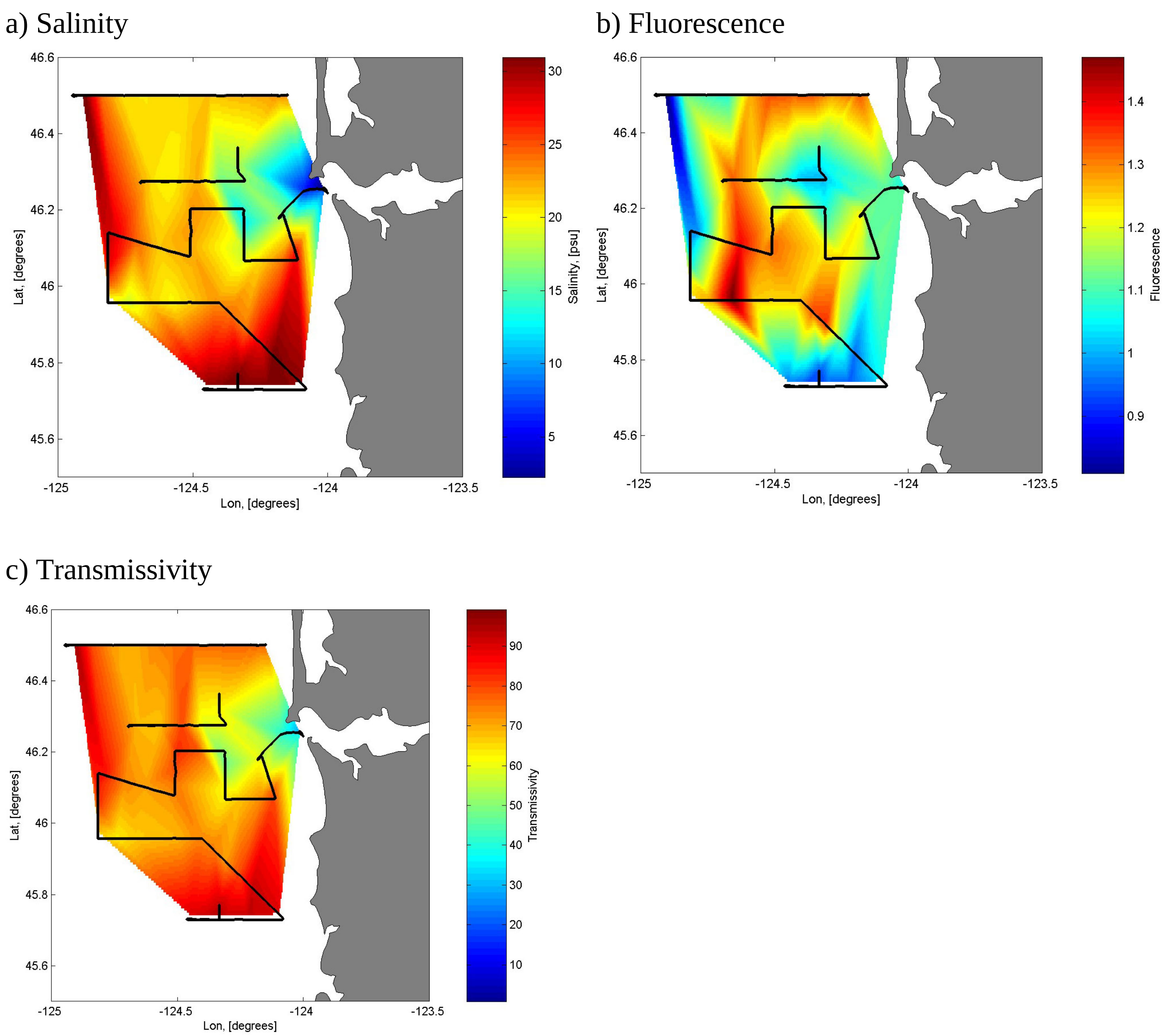

Figure 5: UDAS surface salinity (a),chl-a fluorescence (arbitrary units) (b), and % transmissivity c) c) from the plume drift survey of 7-8 May. New plume water is moving offshore and SW, while old plume water is moving to the south and around the plume, making a "sock"-like structure west of the new plume between 45.9 and 46.2 ºN. Two successive outflow pulses are seen, from a lesser ebb offshore and then a greater ebb near the mouth. These structures are, however, severely aliased by the time required to execute the map. Both new plume water and high salinity coastal water (S ~30) to the south of the plume have little chl-a, whereas old plume water with S ~20-26 is moderately productive.

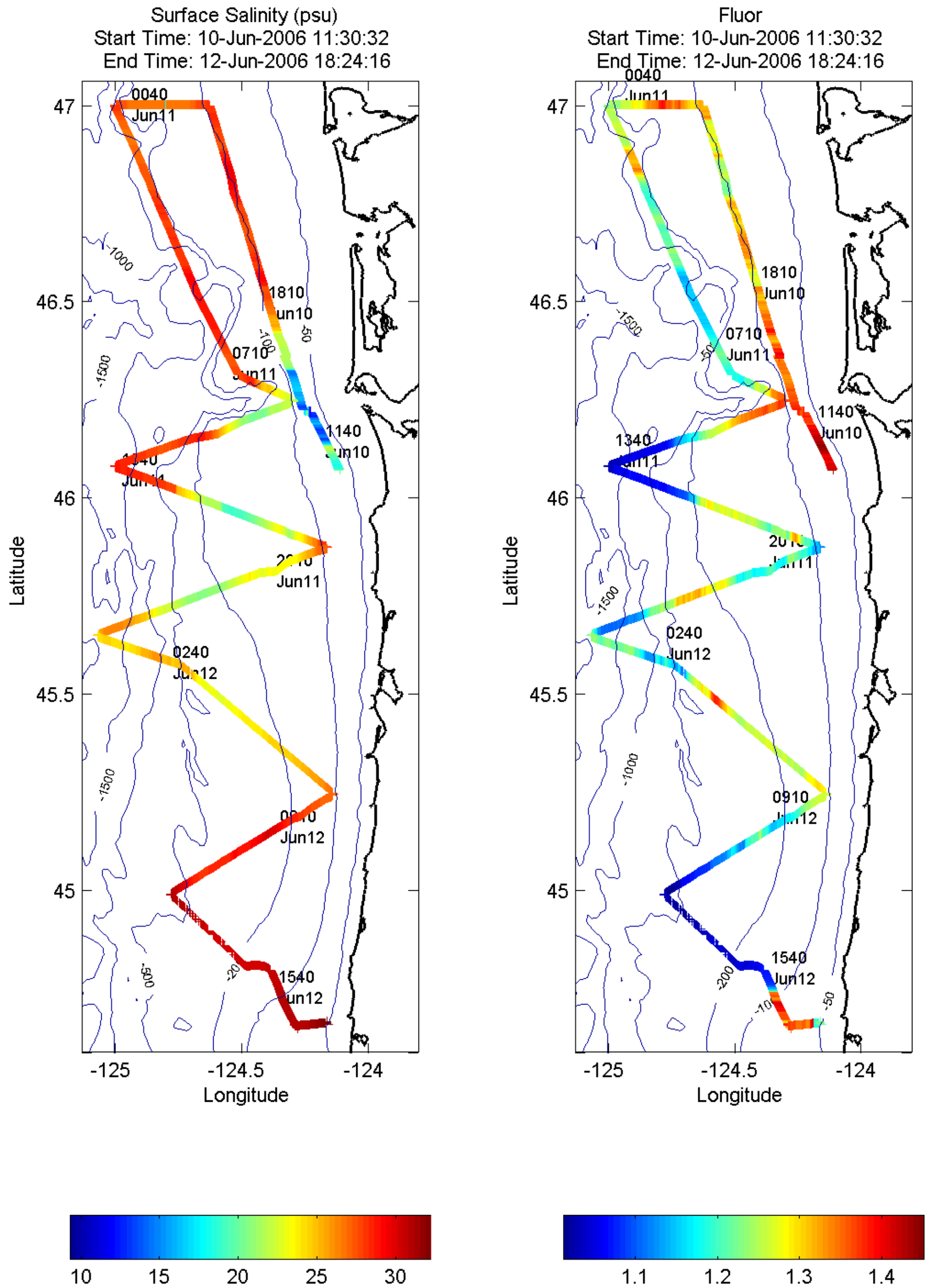

Figure 6: Salinity (left) and chl-a (uncalibrated) from the final map 10-12 June 2006.

d. North and northwestern fronts propagating into lower salinity, older plume waters with considerable ambient stratification. During RISE 4, these fronts seemed to be more successful in spawning soliton trains than either northern or southern fronts, possibly because they propagated with relatively high energy levels into stratified waters. During RISE 4, these waves were found to spawn numerous solitons on every ebb observed, even on weak tides (Figures 7 to 10). Weaker tides break down sooner after high water because the frontal velocity drops below the critical internal Froude number sooner.

e. Southern fronts propagating into stratified, old plume waters with salinities considerably below ambient surface ocean levels. These were found to be very diffuse in 2004 when ambient coastal flow was to the south. They were somewhat sharper this year, when coastal flows were weak or inconsistent, but convergence remained modest, as in 2004.

3. Internal Wave Generation at Plume Fronts

High ambient plume stratification and strong currents coupled with coastal topography provide an environment that is exceptionally rich in internal waves and soliton trains. These internal waves play an important role in plume mixing and may also transport organisms and particles. At least one type of these is directly related to frontal propagation, as observed during RISE 1 in 2004 (Nash and Moum, 2005). Nash and Moum show that soliton trains are spawned when the speed of frontal propagation drops below the intrinsic propagation speed of internal waves in the coastal ocean outside the front. We observed numerous additional examples of this phenomenon during RISE 4 (Figures 7-13). These waves do not, however, form in association with all strong plume fronts, the number of waves formed is highly variable from day to day, different parts of a single front will form variable numbers of waves, and some frontal segments may not release any solitons. Clearly, there is much to understand about these waves.

Figure 7: A northern plume front shown taken 10 June 2006 0330 GMT (evening of 9 June PDT). Note the cuspate structures on several scales. Cusps are much less prominent on stronger fronts.

Figure 8: Several views of the surface expression of a newly-spawned internal soliton spawned from the northern plume front shown in Figure 7, taken 10 June 2006 0400 GMT (evening of 9 June PDT). The first soliton of the packet is in the foreground in each case, but the bottom view represents an earlier stage in soliton evolution than the top two.

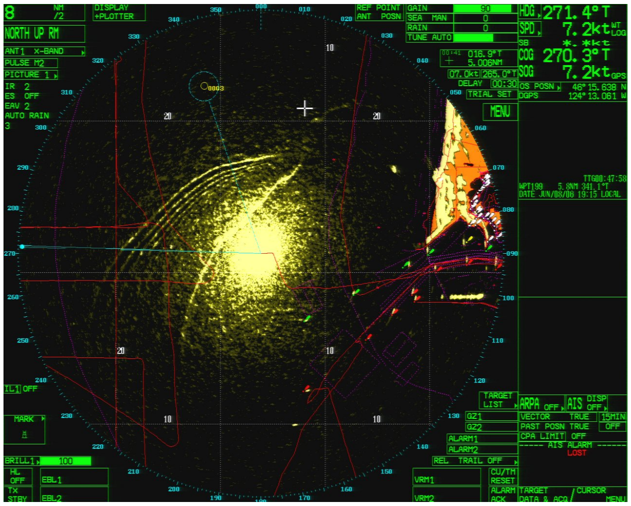

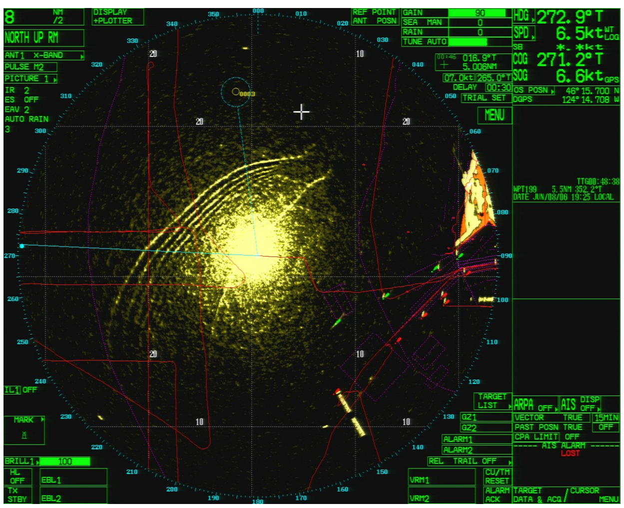

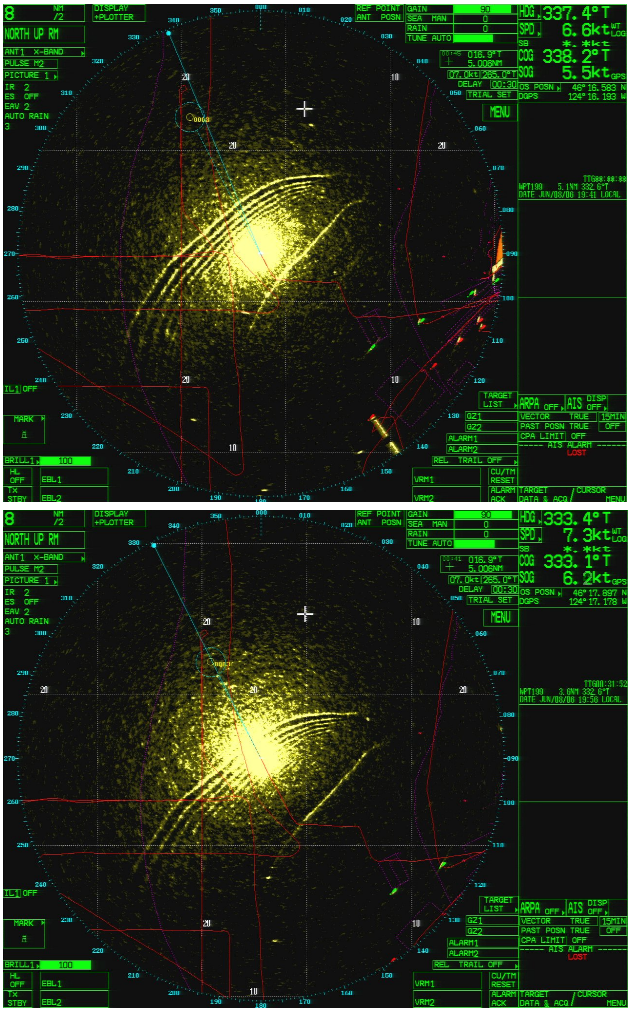

Figure 9: A series of vessel radar images of a group of solitons propagating NW (to the upper left) from a northwestern plume front, the evening of 8 June 2006 from 1900-2000 PDT (9 June, 0300-0400 GMT). At top left, the vessel is just approaching the front. In subsequent images, the vessel crosses the front and moves through the soliton field.

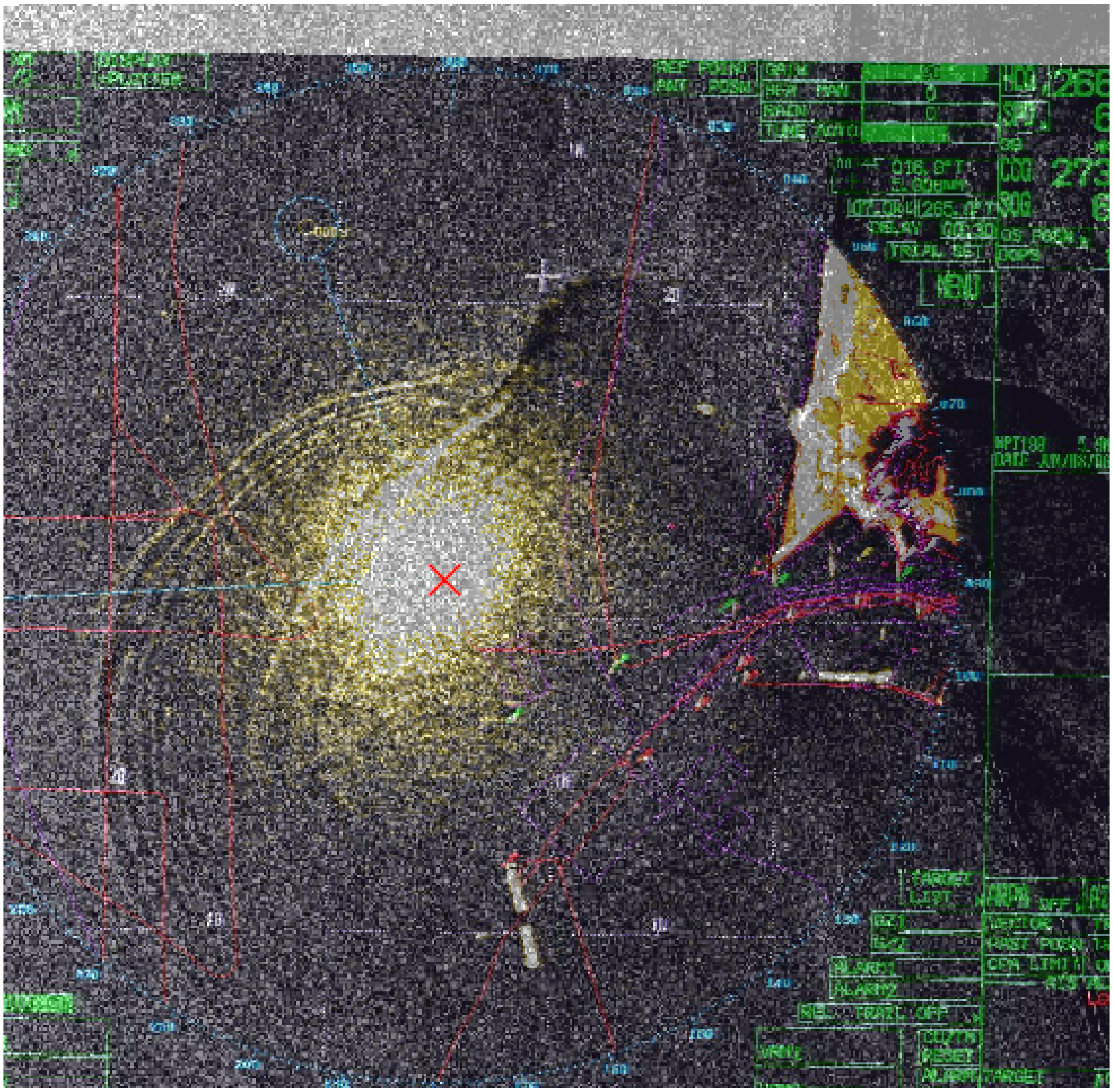

Figure 10: Combined vessel radar and SAR images showing a broader view of the front and associated wave field for the evening of 8 June. The front first breaks down and generates internal waves ("unzips") south of the estuary mouth, so that the distance from the front to the first wave is larger to the south.

The fronts and related waves shown in Figures 7-11 were generated by greater ebbs on the evenings of 8 and 9 June local time; the phenomena for the two evenings exhibit many qualitatively similar features, so are discussed together. Figure 7 shows the primary northwestern front, with a frontal speed of <0.1 m s^{-1} to the NW and a surface convergence (cross-frontal velocity difference) of ~0.3 ms^{-1}, as shown in Figure 10-11. This is not as strong as seen on strong tides, and the front exhibits cuspate features (Figure 7 for 9 June) that render the velocity field complex and 3-D (Figure 10). These cusps are common in less strongly forced fronts (e.g., in Long Island Sound, J. O'Donnell, personal communication). Figure 8 shows the surface signature of the internal waves spawned from the front; the first, fastest moving soliton is moving at ~0.7 m s^{-1}. Figure 9 shows the evolution of the front and associated waves on the evening of 8 June as seen in vessel radar as the vessel passed first through the front and then the waves.

Figure 10 combines vessel radar and SAR (synthetic aperture radar) to broader view of the plume outflow. One interesting feature of Figure 10 is the fact that internal waves are first generated on the south side of the plume, as the front breaks down and then “unzips” south to north. This is related to the sharpening/weakening of the convergence on the north/south sides of the plume, such that the Froude number first becomes subcritical on the south side of the plume. A second unusual feather is the marked bulge of the front to the north, just beyond the point to which the front has unzipped. This bulge is likely related to coastal current patterns, but the details are not obvious.

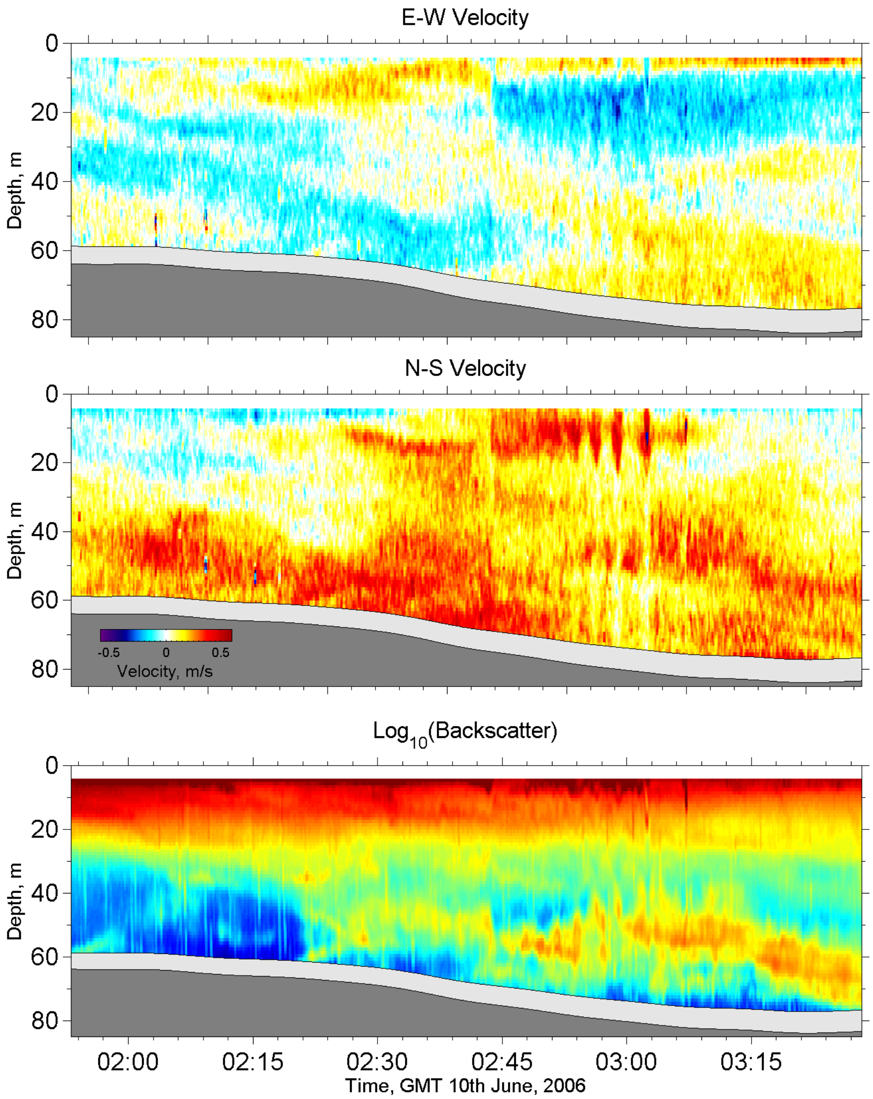

Figure 11: East-west velocity vs. depth (top), north-south velocity vs. depth (middle) and acoustic backscatter vs. depth (arbitrary units, bottom) during a passage (evening of 9 June local time) through a northwest front and waves spawned by this front. Seward is to the right. The frontal crossing is about 0244 GMT, while the waves are seen between ~0250 and 0305.

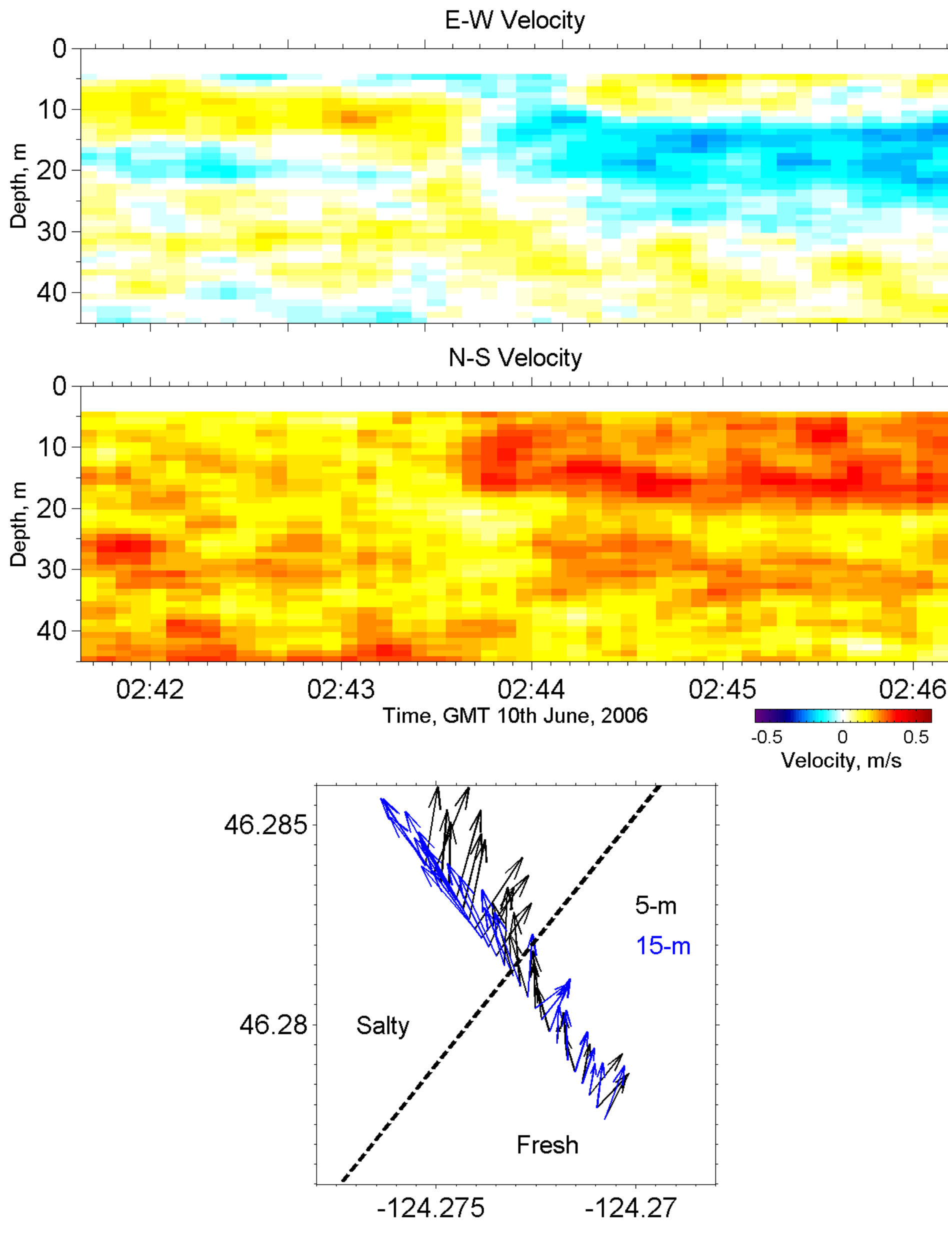

Figure 12: Detail of short-term mean flow (wave flow removed) during a northwestern frontal crossing on greater ebb, evening of 9 June (local time); see Figure 11 for the total flow. Top to bottom: east-west velocity vs. depth, north-south velocity vs. depth, and velocity vectors at 5 and 15 m. The frontal crossing is ~0244.

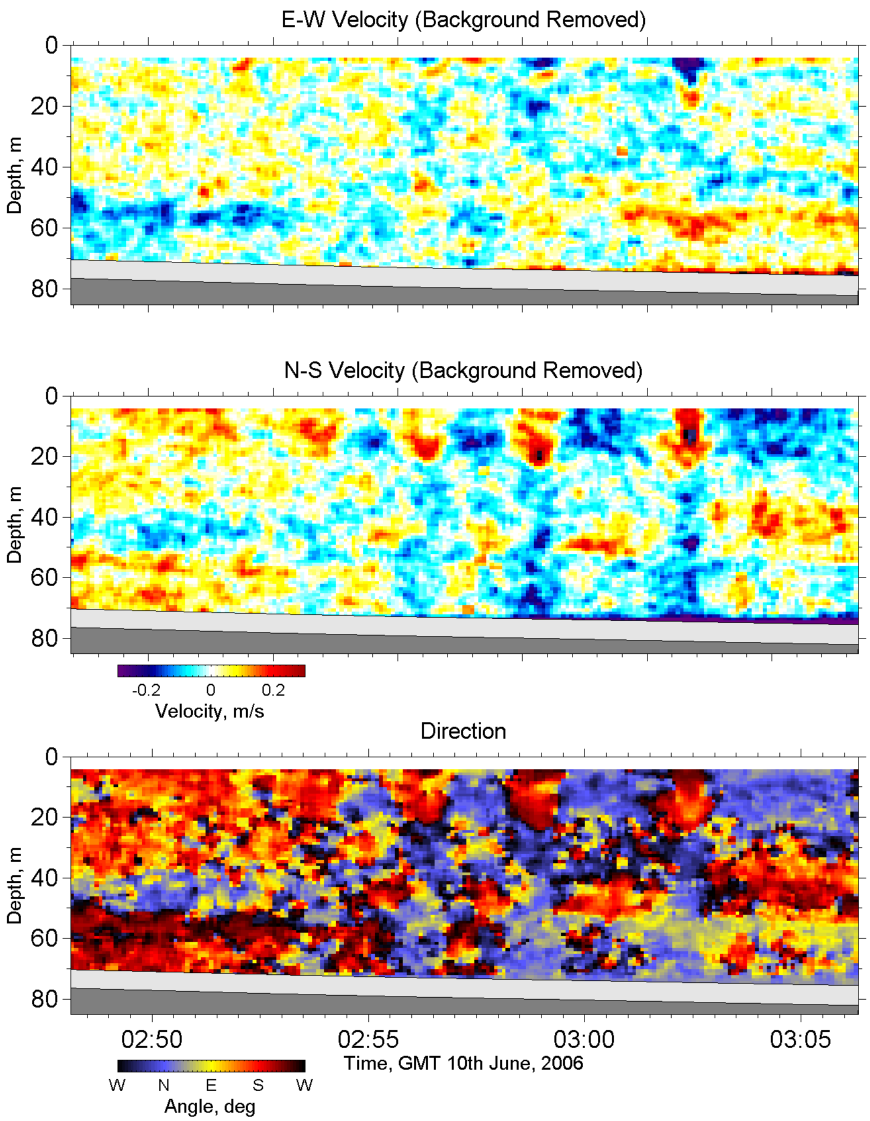

Figure 13: Detail of high-pass filtered flow during a northwest frontal passage, evening of 9 June (local time). From top to bottom: east-west velocity vs. depth, north-south velocity vs. depth, and direction. See Figure 11 for the total flow and Figure 12 for the mean flow near the front, but note difference in time. Four solitons are evident.

Figures 11-13 show (respectively) the total flow, spatial mean flow and wave flow (deviations from spatial mean flow) for a passage through a northwestern plume front and the waves spawned by the front at about 0300 GMT on 10 June. The vessel passes through the front at 0244 GMT (Figures 11-12). The front is sub-critical, having already released solitons. Unlike super-critical fronts, the velocity field around the front is complex and three-dimensional, as evident in the cusps of Figure 7 and in Figure 12. Removal of the mean flow reveals the soliton velocity field (Figure 13). The wave flow in the surface layer is much stronger than that below, but the velocity signature of the waves is evident to the bed at 70 m.

The observations of Figures 11-13 and others during RISE4 suggest the following new information regarding plume fronts and internal wave generation by these fronts:

- The south to north frontal breakdown (unzipping) of the front during wave generation, which occurs when the front becomes subcritical, removes much of the energy of the front, causing it to slow further. Frontal breakdown starts on the south side of the plume, primarily because of the effects of a southward mean flow on the Froude number and perhaps secondarily because of differences in stratification and plume thickness between the north and south sides of the plume.

- Soliton generation occurs closer to the entrance on weaker tides, because the front is moving more slowly on weaker tides, so becomes subcritical sooner.

- The velocity field around the plume front is complex and more 3-D after frontal breakdown.

4. Vertical Mixing

Estimation of vertical turbulent mixing is vital to RISE, because vertical mixing is required to sustain productivity in the stratified waters of the plume region. The plume provides Si and Fe, but usually has little N – in this respect, Figure 6b is more typical than Figure 5b. The N and P needed for primary production are typically provided by upwelled waters. Mixing of plume and upwelled waters brings nutrients and micronutrients (N, P, Si and Fe) together in one water mass, making the plume region highly productive.

A fine-structure, turbulent length-scale analysis enables us to estimate mixing parameters in regions of energetic mixing using CTD density data. On Triaxus, we towed a SeaBird Electronics SBE-9 CTD and two horizontally mounted Ocean Sensors Model OS200 CTDs in a "tow-yo" saw tooth pattern, at horizontal and vertical speeds through water of about 3 m s^{-1} and 1 m s^{-1} respectively. The SBE9 sampling rate was 24 Hz, and the OS200 sampling rate was 9.1 Hz, though the actual sensor response times are similar. The OS200 has a rapid-response integral conductivity-temperature sensor, and was used successfully for detecting density fine-structure overturns in a recent study of Columbia River plume fronts (Orton and Jay, 2005). Here, we present only SBE-9 results, because the SBE-9 has a lower noise levels in density data, and the stratification is weaker than in our previous study. As expected from their relative noise levels, the OS200's typically detected the same overturns as the SBE-9 when they involved large density gradients but no overturns with small density gradients.

In a departure from previous years, we combine vessel 1200 and vessel 300 kHz ADCP to determine isopycnal slopes between Triaxus Seabird CTD passes through the density field (Figure 14). This allows us to discard "pseudo-overturns" – these are inversions in the measured density structure related to low-angle passes through the density field rather than to turbulent overturns. Using this approach, we are now able to estimate vertical mixing by steep internal waves and fronts, as long as the Triaxus path through the density field is not pathological. This approach is not universal – it will only work when density contrasts are large and well resolved in the acoustic backscatter record. However, it is precisely around the energetic structures (fronts and solitons) that are captured very well by the backscatter where we have in past been unable to provide mixing estimates. These structures are near the surface, being centered on the interface between the plume and underlying water. Thus, they are shown very strongly in the backscatter record.

A Thorpe sort is used to restore each measured density vertical profile to a monotonic form, presumable representative of its mean state, unperturbed by transient turbulent eddies. The resulting statistics are used to estimate turbulence parameters. The process of sorting density yields a profile of L, the vertical distance over which each gravitationally unstable density data point has been moved. We compute the Thorpe scale L_T as the rms of L in each overturn patch. Strict quality control methods are used to avoid spurious overturns from measurement noise or from the horizontal movement of the towed platform (Orton and Jay, 2005; Ott et al., 2004). Overturn patches with rms density inversions less than the accuracy of the sensor are also eliminated.

Dissipation of turbulent kinetic energy is estimated as (Thorpe, 1977):

$$\varepsilon = a^2 \overline{L_t^2 \langle N^3 \rangle} \qquad (1)$$

Here, angle brackets denote an average over an overturning patch and the overbar an average over several profiles, and $a \approx 1$. Eddy diffusivity can be computed as (Peters and Johns, 2004):

$$K_\rho = a^2 \Gamma \overline{\langle N \rangle L_T^2} \qquad (2)$$

Here, the mixing efficiency is approximated as $\Gamma \approx 0.22$ for coastal stratified flows (Kay and Jay, 2003; Macdonald and Geyer, 2004).

Preliminary mixing estimates for a greater ebb transect of the N-S Line on the evening of 9 June local time are shown in (Figures 14 and 15). The same transect is used in Figures 7-8 and 11-13. Figure 14 shows the Triaxus CTD path through the backscatter field for a segment of this path. Turbulence estimates (Figure 15) are presented as transect-averages, referenced to depth and density surfaces, with conservative floor and ceiling estimates. The floor is derived from averaging all data, including zeroes where no overturn was observed. The ceiling is derived from averaging all data, but substituting the minimum detectable value wherever no overturn was observed. Sampling lines are defined in Appendix B.

5. Plume-Scale Circulation

Due to strong tides and high river flow, the salinity field near the mouth of the Columbia is highly variable in both space and time. On the ebb, out-flowing river water forms a thin, low-salinity lens that extends out 5 – 20 miles from the mouth on any given ebb pulse. This fresh tongue is bounded by a strong front, with high vertical velocities and frontal vertical and horizontal salinity differences as high as 20 psu. The fresh water in this *inner* plume is less than a day old and was observed to have low fluorescence and salinity between 5 and 20 psu during June 2006. Except during prolonged downwelling periods, the inner plume is surrounded by an *outer* plume with older water. During the June 2006 study, the outer plume was typically

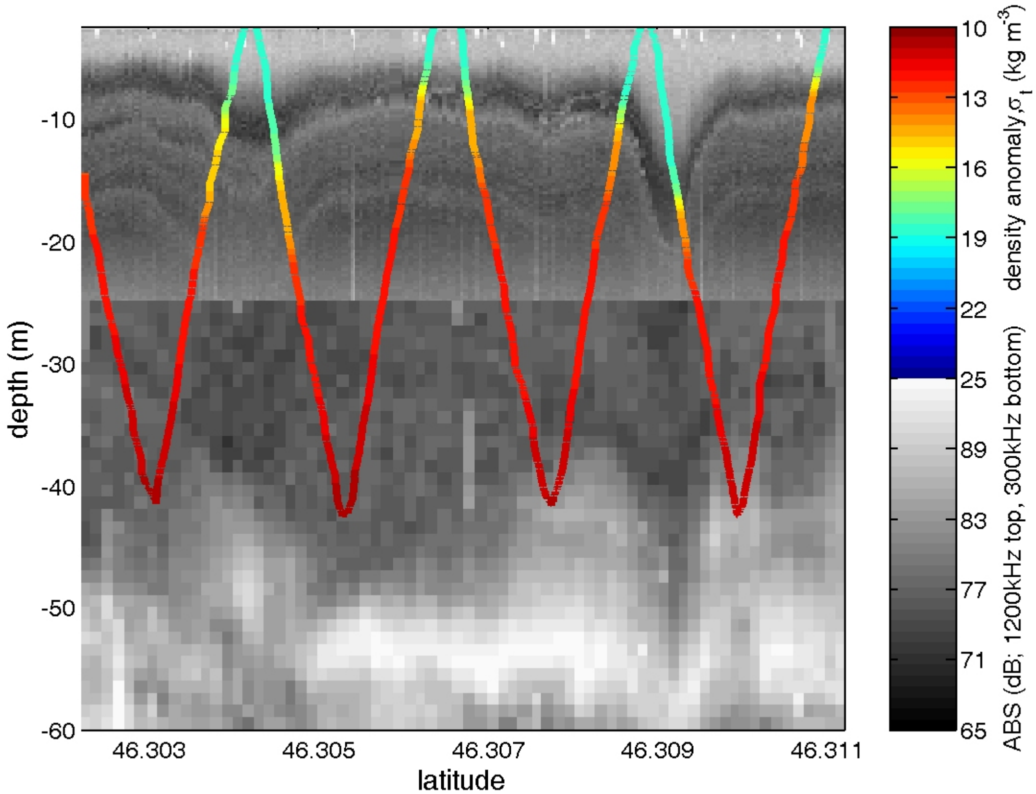

***Figure 14**: Example of passage of Triaxus towfish through the acoustic backscatter field. Acoustic backscatter (greyscale) frequently shows large wave-like undulations in the pycnocline, particularly ahead of fronts. The density colorline from the Triauxus shows these correspond to undulations in the pycnocline. Acoustic backscatter has been used to identify the diapycnal and isopycnal coordinate frame, which is then used in the fine-structure turbulence analysis.*

between 20 and 23 psu and had considerably higher fluorescence than the inner plume. Outer plume water encircled the inner plume and formed a deeper surface later with an interface at ~10mdepth. A snapshot of the plume during upwelling-favorable winds is shown in Figure 5, in which transects near the mouth are chosen such that they are at approximately the same tidal phase.

During upwelling, the front that separates the inner and outer plume spawns internal waves as it slows. These internal waves release energy from the front and transport freshwater into the outer plume. The conversion of inner plume water to outer plume water depends on the partitioning of outflow energy from the estuary. During the June 2006 cruise, the outer plume was strongly stratified and internal waves were emitted frequently from the front. A goal of this work is to understand the transformation of the inner plume to outer plume. The large difference in fluorescence suggests that this will be important to our understanding of the plume ecosystem.

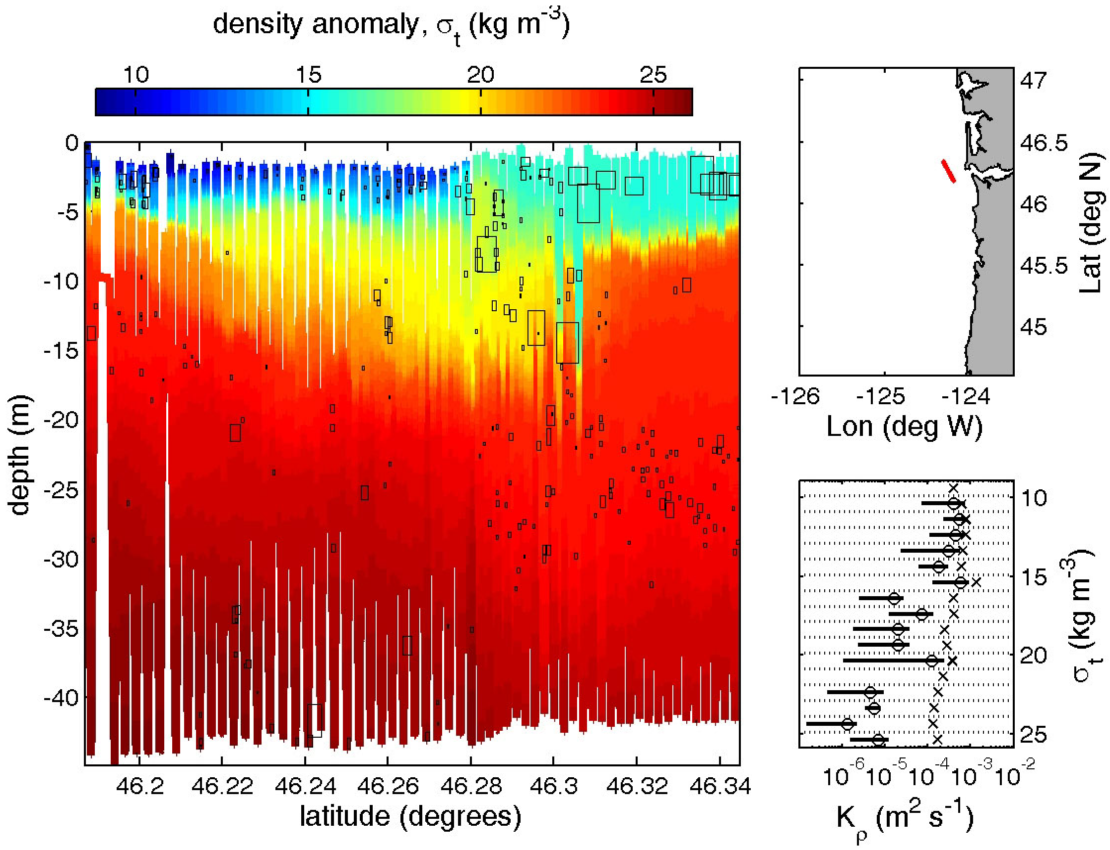

***Figure 15**: Mixing summary diagram from a short cross-mouth transect, 06/10/06 at 0140 - 0335 GMT. At left, density section, with superimposed overturn patches as rectangles. The left side of the rectangle marks the location of the patch in terms of the x-axis. The height of the patch represents the range of depths (and height) for the patch, following the depth scale to the left. The width of the patch represents the Thorpe scale for the patch, also following the y-axis scaling. Regions without boxes are not necessarily lacking overturns; these regions may have a pathological tow path, have failed the quality control tests, or have overturns with a size or density offset below the sensor resolution. At top right: transect map. At bottom right: eddy diffusivity bin-averaged over the transect, in terms of density. Floor (o) and ceiling (+) values are shown, with horizontal lines showing the 95% confidence on the floor value. The mixing computations have uncertainty of less than an order or magnitude only for cases of strong mixing and large vertical density gradients.*

6. Plume Particle Dynamics

Multiple measures of particle properties are available from the RISE sensors: the LISST-100, the LISST-25X, transmissometers on the Triaxus Seabird CTD and the Seabird CTD used for casts, and an optical backscatter sensor (OBS) on the ADCP pipe. Inter-comparison of measurements from these sensors is, therefore, an important issue. Figure 15 shows a comparison between the LISST-25X and a transmissometer resulting from CTD cast RISE4004, which was taken at 0840 GMT on 4 June 2006, in water with salinities that ranged between 31.3 and 32.8. The top two plots, total volume concentration and mean, are taken from the LISST-25X instrument on board the CTD rosette. The bottom two plots show the percentage of light transmission and the depth of the rosette. All the plots are with respect to time. The transmissometer and the mean diameter show a similar trend, which indicates the transmissometer's sensitivity to smaller particle sizes. As we expect, higher volume concentration corresponds to a lower transmission percentage, indicating that we can use both LISST and transmissometer data from the CTD casts, in addition to bottle sample and Triaxus transmissometer data, to analyze particle dynamics.

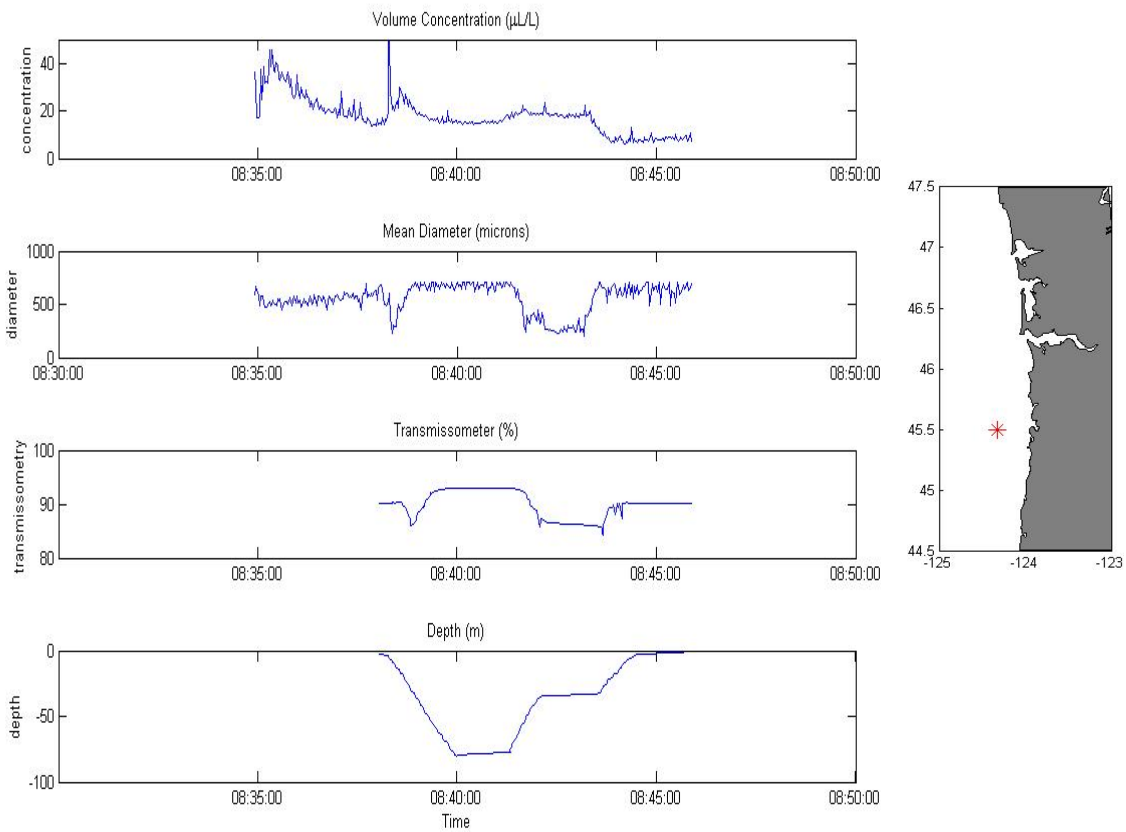

Figure 15: From top to bottom: volume concentration (μl l^{-1}), Sauter mean diameter (μ), % transmissivity. and depth (m) from CTD cast RISE4004.

7. Plankton Distribution

The goal of this project component is to investigate the distribution, abundance, and species composition of mesozooplankton in proximity to the Columbia River plume. The influx of relatively fresh water from the Columbia River plays a role in determining the distribution, abundance and biovolume of plankton over the continental shelf. Transects north, south and adjacent to the Columbia River were used to assess regional variations in proximity to the river.

Northern Shelf

The northernmost transect repeated during the survey was on the Long Beach (LB) line at 46º 30’ N (Figure 16). Data from the Laser Optical Plankton Counter (LOPC) and its associated CTD and fluorometer provide detailed information on the influence of river plume intrusions on plankton in the region. The salinity profile along the LB transect depicts a recent intrusion of fresh water centered within aged plume waters. The fresher (S <20), new plume waters are noticeably lacking in chlorophyll compared to the intermediate salinity (20-25) waters on either side (Figure 1). High abundances of plankton are evident along the bottom margin of the low salinity plume waters, as well as throughout the upper 40 m of the water column in the nearshore region.

Plankton biovolume (Figure 16) was greatest offshore and indicates that the inshore zooplankton were much smaller than offshore. The transect was sampled during darkness and the high biovolume/low abundance evident in the offshore region is likely a function of vertically migrating krill that come to the surface at night to feed.

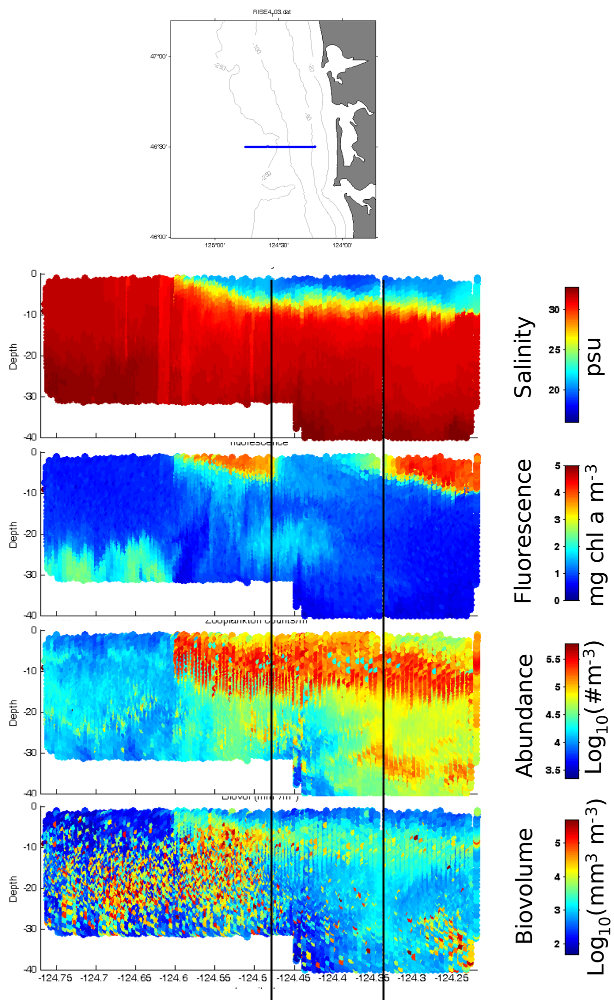

Figure 16: The distribution of salinity, fluorescence, plankton counts and plankton biovolume along the Long Beach (LB) line north of the Columbia River. The 2 vertical lines depict the region with the freshest overlying “new plume” wa-

The Columbia River Transect

Off the mouth of the Columbia River, a freshwater surface plume is quite evident during the ebb tide. A similar pattern to that mentioned for the Northern shelf region exists off the mouth of the Columbia River. Within the lowest salinity water, indicative of "new plume" water, of the freshwater plume where convergence of water masses leads to downwelling of surface waters. The depression of the surface waters is strongest along the northern edge of the plume.

Southern shelf

Repeated transects along the southern shelf were not performed during this study due to some initial equipment problems. At the end of the cruise, a large-scale survey was conducted from Gray's Harbor (47º N) down to Newport, OR (44.6º) with several transects across the continental shelf (Figure 17). The salinity at 2 m depth depicts the distribution of the freshwater plume flowing towards the southwest from the Columbia River mouth. Elevated levels of chl a appear to be primarily concentrated along the shelf break at the 250 m isobath. Higher abundances of zooplankton are evident along the Oregon shelf associated with the outer margins of the plume.

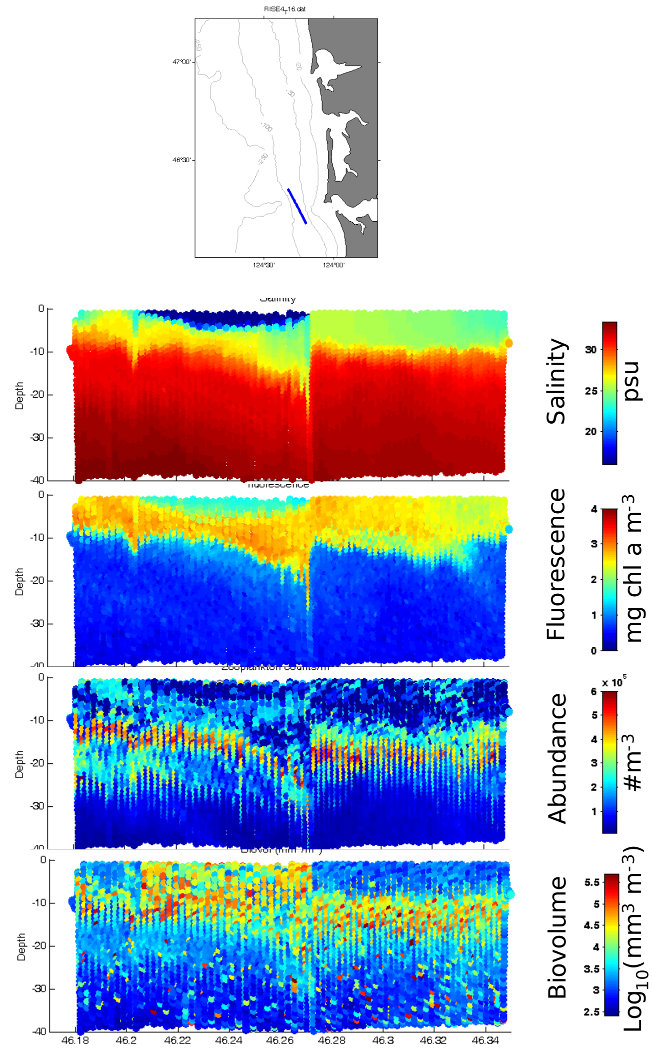

Figure 17: The distribution of salinity, fluorescence, plankton counts and plankton biovolume off the Columbia River. The 2 vertical lines depict the region with the freshest overlying "new plume" waters.

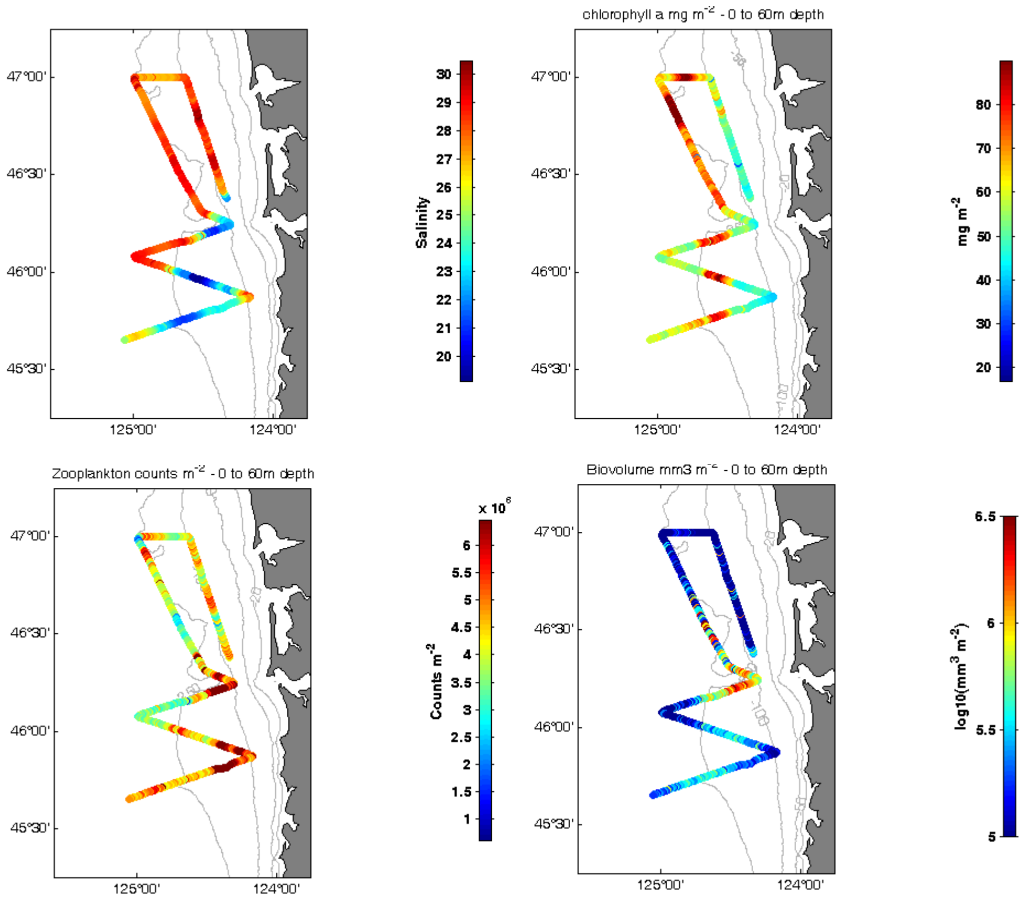

Figure 18. Plots of salinity (2 m depth), and 0 – 60 m integrated chl a fluorescence, zooplankton abundance and biovolume across the study area.

References

Kay, D.J., and D.A. Jay (2003), Interfacial mixing in a highly stratified estuary 1: Characteristics of mixing, *J. Geophys. Res.*, 108(C3), 3072, doi:10.1029/2000JC000252.

Klymak, J.M., and M.C. Gregg (2004), Tidally generated turbulence over the Knight Inlet sill, *J. Phys. Oceanogr.*, 34, 1135-1151.

Macdonald, D.G. and Geyer, W.R., 2004. Turbulent Energy Production and Entrainment at a Highly Stratified Estuarine Front. *Journal of Geophysical Research* 109, C05004, doi: 10.1029/2003JC002094.

Nash, J. D. and J. N. Moum, 2005, River plumes as a source of large amplitude internal waves in the ocean, in press, *Nature*.

Orton, P. M. and D. A. Jay, 2005, Observations at the tidal plume front of a high-volume river outflow, in press, *Geophys. Res. Let*.

Ott, M.W., J.A. Barth, and A.Y. Erofeev (2004), Microstructure measurements from a towed undulating platform, *J. Atmos. Oceanic Technol.*, 21, 1621-1632.

Thorpe, S.A. 1977. Turbulence and mixing in a Scottish loch. Philos. Trans. R. Soc. London A, 286:125-181.

Appendix A: Rise 4 Transects

name	startdate	starttime utc	enddate	endtime utc	startlon	startlat	endlon	endlat	meanCOG deg from N
Initial Map									
tran0602_01	2-Jun-06	16:28:20	2-Jun-06	17:16:12	-124.05	44.6273	-124.168	44.6379	277.628
tran0602_02	2-Jun-06	17:16:48	2-Jun-06	19:26:24	-124.17	44.639	-124.223	44.619	240.8174
tran0602_03	2-Jun-06	19:27:00	2-Jun-06	19:43:40	-124.223	44.6199	-124.191	44.6518	34.8409
tran0602_04	2-Jun-06	19:44:16	2-Jun-06	20:34:40	-124.191	44.6525	-124.277	44.6525	270.2537
tran0602_05	2-Jun-06	20:53:40	2-Jun-06	23:47:56	-124.328	44.6527	-124.545	44.6174	257.2287
tran0602_06	2-Jun-06	23:48:32	3-Jun-06	0:29:00	-124.544	44.618	-124.458	44.6522	60.2478
tran0603_01	3-Jun-06	1:25:32	3-Jun-06	2:50:00	-124.455	44.657	-124.58	44.6441	261.8961
tran0603_02	3-Jun-06	2:50:36	3-Jun-06	11:11:24	-124.581	44.6445	-124.022	45.4958	24.914
tran0603_03	3-Jun-06	12:53:44	3-Jun-06	16:32:40	-123.999	45.4975	-124.115	45.4851	261.3576
tran0603_04	3-Jun-06	16:33:16	3-Jun-06	17:57:44	-124.115	45.4852	-124.061	45.4941	77.2167
tran0603_05	3-Jun-06	17:58:20	3-Jun-06	20:43:12	-124.061	45.4947	-124.128	45.4849	258.2729
tran0603_06	3-Jun-06	21:03:28	3-Jun-06	22:00:00	-124.064	45.4975	-124.108	45.4933	262.6508
tran0603_07	3-Jun-06	22:01:08	3-Jun-06	22:46:24	-124.109	45.4935	-123.997	45.4943	88.8434
tran0603_08	3-Jun-06	22:47:00	4-Jun-06	12:28:40	-123.997	45.4954	-124.72	45.491	269.1373
tran0604_01	4-Jun-06	12:28:40	5-Jun-06	1:07:48	-124.72	45.491	-124.016	46.256	33.1992
tran0605_01	5-Jun-06	1:08:24	5-Jun-06	2:00:08	-124.016	46.2563	-124.154	46.2812	285.1936
tran0605_02	5-Jun-06	2:00:44	5-Jun-06	3:20:28	-124.154	46.2826	-124.117	46.4959	6.9321
LB Line									
tran0605_03	5-Jun-06	3:21:04	5-Jun-06	9:05:32	-124.117	46.4975	-124.767	46.5015	270.4647
tran0605_04	5-Jun-06	9:06:04	5-Jun-06	12:27:12	-124.767	46.5004	-124.214	46.5002	90.1233
tran0605_05	5-Jun-06	12:27:48	5-Jun-06	15:30:28	-124.214	46.5012	-124.753	46.5012	270.126
tran0605_06	5-Jun-06	15:31:04	5-Jun-06	16:34:44	-124.753	46.5022	-124.59	46.4986	91.9091
tran0605_07	5-Jun-06	16:35:20	5-Jun-06	18:09:52	-124.59	46.4974	-124.875	46.5001	270.9378
tran0605_08	5-Jun-06	18:10:28	5-Jun-06	22:23:20	-124.875	46.5012	-124.217	46.4988	90.1976
tran0605_09	5-Jun-06	22:23:56	6-Jun-06	2:11:44	-124.218	46.4997	-124.836	46.5006	270.1161
tran0606_01	6-Jun-06	2:12:20	6-Jun-06	5:55:56	-124.836	46.5015	-124.214	46.5002	90.0608
tran0606_02	6-Jun-06	5:56:32	6-Jun-06	10:21:48	-124.213	46.5013	-124.946	46.5002	269.8889
tran0606_03	6-Jun-06	10:22:24	6-Jun-06	15:06:20	-124.946	46.499	-124.201	46.4999	90.0431
tran0606_04	6-Jun-06	17:19:08	6-Jun-06	23:48:12	-124.102	46.5004	-124.916	46.5004	270.1061
tran0606_05	6-Jun-06	23:48:48	7-Jun-06	4:23:04	-124.916	46.5013	-124.213	46.5001	90.0605

tran0607_01	7-Jun-06	4:23:40	7-Jun-06	7:04:24	-124.213	46.5003	-124.33	46.5278	288.0647
Plume Drift map									
tran0607_02	7-Jun-06	7:05:00	7-Jun-06	9:42:40	-124.33	46.5267	-124.256	46.2501	169.5538
tran0607_03	7-Jun-06	9:43:16	7-Jun-06	10:53:32	-124.256	46.2491	-124.467	46.2372	265.1574
tran0607_04	7-Jun-06	10:54:04	7-Jun-06	12:15:40	-124.467	46.236	-124.284	46.1573	121.7116
tran0607_05	7-Jun-06	12:16:16	7-Jun-06	13:11:36	-124.284	46.1584	-124.295	46.2718	355.6804
tran0607_06	7-Jun-06	13:12:12	7-Jun-06	15:31:32	-124.296	46.2731	-124.697	46.2728	269.8592
tran0607_07	7-Jun-06	15:32:08	7-Jun-06	17:51:56	-124.696	46.2715	-124.307	46.2767	88.683
tran0607_08	7-Jun-06	17:52:32	7-Jun-06	18:47:12	-124.308	46.2779	-124.33	46.3686	349.6245
tran0607_09	7-Jun-06	18:47:48	8-Jun-06	0:06:32	-124.332	46.3689	-124.334	45.7307	180.2228
tran0608_01	8-Jun-06	0:07:08	8-Jun-06	0:52:28	-124.335	45.7299	-124.462	45.7309	270.8681
tran0608_02	8-Jun-06	0:53:04	8-Jun-06	3:09:20	-124.462	45.7319	-124.081	45.7308	90.0734
tran0608_03	8-Jun-06	3:09:52	8-Jun-06	6:09:24	-124.081	45.7319	-124.403	45.9568	315.0486
tran0608_04	8-Jun-06	6:10:00	8-Jun-06	8:39:48	-124.404	45.957	-124.815	45.9572	270.293
tran0608_05	8-Jun-06	8:40:24	8-Jun-06	10:31:32	-124.816	45.9579	-124.815	46.1386	0.30009
tran0608_06	8-Jun-06	10:32:08	8-Jun-06	12:25:44	-124.814	46.1394	-124.511	46.0791	105.8416
tran0608_07	8-Jun-06	12:26:20	8-Jun-06	13:36:56	-124.511	46.0799	-124.511	46.2001	359.9385
tran0608_08	8-Jun-06	13:37:32	8-Jun-06	14:51:20	-124.51	46.2013	-124.313	46.2023	89.6841
tran0608_09	8-Jun-06	14:51:56	8-Jun-06	15:48:32	-124.312	46.2011	-124.31	46.0676	179.2817
tran0608_10	8-Jun-06	15:49:08	8-Jun-06	16:58:44	-124.309	46.0667	-124.113	46.068	89.2915
tran0608_11	8-Jun-06	16:59:20	8-Jun-06	18:10:08	-124.112	46.0688	-124.165	46.1864	342.1953
RT to Astoria									
N-S Line									
tran0608_12	8-Jun-06	22:18:56	8-Jun-06	23:14:52	-123.824	46.1913	-124.007	46.2499	295.0426
tran0609_01	9-Jun-06	1:01:56	9-Jun-06	2:30:00	-124.017	46.2554	-124.257	46.262	272.4153
tran0609_02	9-Jun-06	2:30:36	9-Jun-06	3:33:40	-124.258	46.2623	-124.328	46.3511	331.5309
tran0609_03	9-Jun-06	3:34:16	9-Jun-06	5:02:20	-124.327	46.35	-124.2	46.1809	152.5135
tran0609_04	9-Jun-06	6:19:04	9-Jun-06	8:17:28	-124.207	46.1787	-124.328	46.3521	333.851
tran0609_05	9-Jun-06	8:18:04	9-Jun-06	10:04:00	-124.33	46.3511	-124.201	46.1782	152.6877
tran0609_06	9-Jun-06	10:04:36	9-Jun-06	11:59:24	-124.199	46.1786	-124.326	46.3498	332.5014
tran0609_07	9-Jun-06	12:00:00	9-Jun-06	15:15:36	-124.328	46.3491	-124.097	46.0859	148.8135
tran0609_08	9-Jun-06	15:16:12	9-Jun-06	20:02:00	-124.096	46.0853	-123.827	46.1915	59.7664
RT to	**Astoria**								
tran0610_01	10-Jun-06	0:04:24	10-Jun-06	1:40:12	-123.942	46.2069	-124.193	46.1844	262.7729
tran0610_02	10-Jun-06	1:40:48	10-Jun-06	3:35:28	-124.194	46.1836	-124.326	46.3523	NaN

tran0610_03	10-Jun-06	3:36:04	10-Jun-06	6:20:40	-124.325	46.3535	-124.106	46.0642	NaN
tran0610_04	10-Jun-06	6:21:16	10-Jun-06	9:45:48	-124.104	46.0648	-124.324	46.3529	332.114
tran0610_05	10-Jun-06	9:46:24	10-Jun-06	12:22:16	-124.325	46.3524	-124.112	46.0691	152.6252
tran0610_06	10-Jun-06	12:22:52	10-Jun-06	15:22:32	-124.113	46.068	-124.328	46.3507	332.2102
Final Map									
tran0610_07	10-Jun-06	16:48:16	11-Jun-06	1:02:40	-124.323	46.3574	-125	47.0002	NaN
tran0611_01	11-Jun-06	1:03:16	11-Jun-06	8:56:48	-125.001	46.9995	-124.296	46.2456	NaN
tran0611_02	11-Jun-06	8:57:24	11-Jun-06	13:27:36	-124.297	46.2444	-125.003	46.0782	251.237
tran0611_03	11-Jun-06	13:28:12	11-Jun-06	18:50:52	-125.003	46.0771	-124.162	45.8723	109.2994

Appendix B: Sampling Plans

These maps were compiled for planning purposes. Deviations from planned courses occurred frequently, due to such factors as traffic, sea conditions, and crab-pot concentrations. Some planned lines were honored in the breach rather than the observation. Also, lines like the NS-Line were repeated multiple times. The scale is not constant in the following maps, which are for illustrative purposes only.

1. Final Plume Map:

2. The Long Beach Line

3. <u>Inner Plume Sampling Lines</u>:

The NS-Line in original form:

The NS-Line, modified to avoid crab pots: